We are IntechOpen,
the world's leading publisher of
Open Access books
Built by scientists, for scientists

5,800
Open access books available

142,000
International authors and editors

180M
Downloads

Our authors are among the

154
Countries delivered to

TOP 1%
most cited scientists

12.2%
Contributors from top 500 universities

CLARIVATE ANALYTICS
BOOK CITATION INDEX
INDEXED

WEB OF SCIENCE™

Selection of our books indexed in the Book Citation Index
in Web of Science™ Core Collection (BKCI)

Interested in publishing with us?
Contact book.department@intechopen.com

Numbers displayed above are based on latest data collected.
For more information visit www.intechopen.com

Defect Detection in Delaminated Glass-Fibre/Epoxy Composite Plates Using Local Defect Resonance Based Vibro-Thermography Technique

Subhankar Roy and Tanmoy Bose

Abstract

In the present scenario, composites are widely used for various applications in the field of aerospace, automobile, marine, sports, construction and electrical industries. The need of damage inspection for these composite structures has been of great importance. Complicated defects like delaminations present in the composite laminates can be detected effectively using nonlinear acoustic wave spectroscopy (NAWS). One of the NAWS techniques of detecting the delamination is based on intensification of vibration amplitudes at the delamination location, known as local defect resonance (LDR) technique. In this chapter, a numerical investigation for detecting delamination in glass fibre reinforced polymer (GFRP) composite based on vibrothermography technique will be discussed. A single periodic LDR frequency excitation is used to excite the GFRP plate, resulting in a local temperature rise at delamination region due to frictional heating at the damage interface. An explicit dynamic temperature displacement analysis will be carried out for a specific time period of LDR excitation. Subsequently, a heat transfer analysis will be performed to observe the temperature difference at top surface of the delaminated GFRP plate. Thus a numerical investigation will be carried out based on LDR excitation for high contrast imaging of delamination in composite materials using vibro-thermography.

Keywords: local defect resonance (LDR), delamination, vibro-thermography, frictional heating, glass fibre reinforced polymer (GFRP)

1. Introduction

In recent times, composite materials finds a wide variety of applications in several fields of engineering such as automobile, aerospace, building materials, etc. because of their good strength to weight ratio, higher resistance to impact, better fatigue property and lower costs. The composite materials are generally classified into three vast categories according to their matrix material type, namely, polymer matrix composites (PMCs), metal matrix composites (MMC) and ceramic matrix composites (CMCs). The Glass fibre reinforced polymer (GFRP) and carbon fibre

reinforced polymer (CFRP) represents the largest class of polymer matrix composites (PMCs) which find numerous applications in the fabrication of aerospace structures, turbine blades, automobile skin, etc. These structures are continuously subjected to various cyclic loads and impacts during the tenure of their service and hence may lead to development of damages in their sub-surface layers, in form of delamination. So, this chapter will discuss a technique of determining the location of such delaminations by performing vibro-thermography based on local defect resonance of the defect. The vibro-thermography technique is an efficient technique for determining the location of damage in a complex structure by exciting the structure at its defect frequency, known as the local defect resonance frequency. Excitation at the defect frequency leads to high amplitude vibration at the defect site resulting in clapping action of the layers, thus, generating a local heat at the defect area. This temperature gradient in the defect area can be easily detected using an IR-camera.

The vibro-thermography technique was implemented by many researchers in the past for carrying out non-destructive evaluation of defects in structures. Vibro-thermography was first introduced by for the detection of subsurface damages in composite structures due to fatigue [1]. They studied the elastic and viscoelastic hysteretic effects by mechanically exciting the specimen and obtaining the thermal patterns. It was observed that the material deformation during the excitation was directly related to the heat generated. The study was further implemented by using resonant vibration to obtain high cyclic stresses [2]. In the year 1996, Rantala et al. excited a sample with mechanical shaker and monitored the sample with an infrared camera to perform a lock-in thermography technique [3]. The high amplitude of vibration led to high temperature signatures at low stress levels which is very good for non-destructive evaluation. Another study used lock-in thermography based on optical heating of defect area for large area inspections [4]. Subsequently, a short pulse sound was used in addition to IR imaging to measure surface temperature as a function of time [5]. This led to efficient detection of subsurface cracks due to enhancement of sonic infrared imaging. Vibro-thermography was found to be an outstanding tool for fast detection of small defects like cracks and delaminations [6]. It was observed that the defect can be detected from any side inspection and not required for all-side inspection. Also, a single excitation location is sufficient to perform a large area scanning and is found very useful for composites with multiple materials having different thermal properties. The vibro-thermography technique was also implemented for determining the size of a defect [7]. In this study, a numerical model was developed using finite difference method where it was observed that the size of defect influences phase angle data, thus affecting the defect depth estimation. In the following year, the lock-in thermography technique was used to differentiate between location, shape and size of defects in case of cracks and corrosion defect [8]. Subsequently, the lock-in thermography was implemented for detection of vertical cracks of arbitrary shape to determine geometry and location of defect [9]. An algorithm is developed to obtain crack shape reconstructions by optimizing the data before entering the algorithm. Deep cracks are precisely detected although the shape of the crack is obtained as rounded and having a slightly over-estimated area. Another group of researchers investigated novel hybrid thermographic techniques in addition to traditional optically excited thermography using external optical radiation such as heaters, flashes and laser systems [10]. Different techniques such as ultrasonic stimulated thermography with ultrasonic waves and damage resonance to enhance the sensitivity of micro-cracks; microwave thermography that uses electromagnetic radiation at microwave frequency bands; and eddy current stimulated thermography to generate induction heating is used for detection of delaminations and cracks. Subsequently, an

integrated nonlinear ultrasound and Vibro-thermography based non-destructive testing was proposed using shared excitation sources to solve low sensitivity and small detection area problems in carbon fibre reinforced polymer structures [11]. The study involved time-domain analysis and fast Fourier transform of image sequences obtained from specimens with different impact loads. In case of visible damages, FFT did not improve the sound to noise ratio although the location and shape of the defect were captured in detail. On the other hand, the barely visible impact damages were only detected using nonlinear ultrasound and vibro-thermography technique due to a better sound to noise ratio. Non-destructive testing of CFRP with impact damages using ultrasonic simulation was further implemented using two approaches: low power resonant ultrasonic stimulation and high power stimulation at a fixed frequency [12]. The high power ultrasonic IR thermography using magnetostriction and piezoelectric transmitters proved to be highly informative but at the same time, ultrasonic IR testing needs a higher level of energy consumption in order to induce temperature signatures of desired amplitude. In contrast, low power ultrasonic stimulation using defect resonance allows investigation of complex structured flaws like impact damages while reducing the energy consumption to half when compared with high power ultrasonic thermography. The study was extended by the same group where it is shown that small deviations in the frequency of acoustic signal supplied to transducer from frequency of main resonance leads to a reduction in radiation intensity and thus decreases in temperature at defect location [13]. Hence, the transducer must operate at its resonant frequency for effective ultrasonic stimulated thermography.

Furthermore, a modelling scheme was developed to simulate vibro-thermography of structures used in gas turbine engine components in order to reduce mass and enhanced cooling [14]. The framework of the model is comprised of coupled thermoplastic heat generation and various effects due to nonlinear vibration arising from excitation, engagement force on target structure by the ultrasonic horn, and structural boundary conditions. It has been observed from contact dynamic simulations that subharmonics, superharmonics, sub-superharmonic and chaos are all present in the structure even if the exciter is sharply tuned at the resonant frequency. This model is also used for obtaining spatio-temporal temperature distribution in the target structure that can be extended to understand vibro-thermographic characteristics in complex structures with hidden defects. Subsequently, a significant increase in SNR combined with suppression of effects due to non-uniform heating, background reflections and surface non-uniformities can be achieved by a novel adaptive spectral band integration procedure for post-processing of flash thermography data [15]. This procedure integrates spectral information of each individual pixel thus obtaining maximum detectability of defects such as flat bottom holes, BVIDs as well as a stiffened composite panel with production defects. The technique was also able to estimate the accurate size and depth of the defects when compared with pulsed phase thermography. Moreover, the same group of researchers compared the efficiency of time and frequency domain analysis techniques in flash thermography to improve the detectability of defects [16]. Single bin procedures such as thermal signal area and dynamic thermal tomography; and integrated bin procedures such as frequency domain tomography and adaptive spectral band integration are considered for the study. The single bin approach in the frequency domain showed better detectability of defect and higher defect depth estimation as compared to its time domain counterpart. Further, the integrated frequency domain approach shows higher sensitivity to non-uniform heating and the best defect detectability among all.

Subsequently, nonlinear acoustic wave spectroscopy (NAWS) has recently proved to be an efficient tool for detection of small defects in structures [17]. NAWS has an advantage over conventional non-destructive testing (NDT) techniques where the information about reflection of incident vibration waves play a major role in in detection of damages [18]. The interaction between defect and the incident wave leads to generation of higher harmonics which can be better understood using NAWS [19]. Local defect resonance (LDR) phenomenon is one of such NAWS technique that is emerging in recent years. Since the scattering and reflection data of the incident signal in case of smaller defects is not so prominent, NAWS and vibro-thermography technique are combined for detection of defects [20]. LDR based vibro-thermography technique is much advantageous and less time consuming than other NDT techniques for detection and location of small defects even in intricate structures. Moreover, the LDR based frictional heating was introduced which illustrated the rubbing and clapping action at defect site induces an internal heating that can be detected easily using an IR camera [21]. It was observed that the amplitude of vibration is quite high at the defect location when excited with its fundamental defect frequency. Subsequently, an IR camera was used with cell phone attachment for performing lock-in thermography [22]. With the help of image processing, sub-surface defects and dental caries were successfully detected. Also, a LDR based thermal imaging experiment was carried out to characterize various defects using air-coupled ultrasound excitation [23]. Further, defects were successfully activated using sweep excitation for low energy vibro-thermography technique [24]. The post-processing included a Fourier-transform of the temperature response obtained from the defect in case of unknown LDR frequencies. The LDR concept was also used in combination of IR imaging for detecting minute defects using a nonlinear ultrasonic stimulated thermography (NUST) method [25]. It is found that by exciting the structure at a frequency yielding nonlinear response may lead to increase in the temperature rise at defect area. The same research group again used sweep excitation for activating the LDR frequency in order to obtain higher heat generation at a crack surface [20].

The various literatures discussed on vibro-thermography and LDR based vibro-thermography suggests that the technique is widely accepted for detection, location and sizing of defects in composite structures. The advantage of such a technique is mainly for detection of small and complicated defects such as delaminations and barely visible impact damages (BVIDs) in composite structures. Hence, this chapter will address the problem of defect detection in glass fibre reinforced polymer (GFRP) composite by implementing LDR based vibro-thermography technique.

2. Theory

2.1 Local defect resonance (LDR)

The local defect resonance (LDR) is a phenomenon that occurs mainly due to presence of a defect in any structure. Whenever, a structure consists of damage, the local stiffness and mass of the structure at defect location changes. This change leads to a new parameter known as the effective stiffness and effective mass of the structure over the defect area. According to Solodov et al. [21], when the plate with defect is excited with a frequency that matches with the frequency of the defect due to its effective stiffness and effective mass, resonance occurs. This phenomenon of resonance at the defect area is termed as local defect resonance. The LDR phenomenon leads to high amplitude of vibration at the defect location while the rest of the plate remains at negligible amplitudes. Exciting a plate with one of its LDR

frequency will lead to clapping and rubbing action at the corresponding defect. This clapping and rubbing action will further generate a local heat over the damage area. The analytical relation for detection of LDR frequency is given by Solodov et al. [21], in case of a flat bottom hole, which can be found analogous to a case of delamination in composites.

Figure 1 shows a schematic of four layered composite with central delamination. The analytical relation for calculating LDR frequency is based on parameters such as diameter of delamination (a) and residual thickness (t). The effective stiffness (K_e) of the structure at defect location is given by [26]

$$K_e = \frac{64\pi E t^3}{a^2(1-\nu^2)} \tag{1}$$

Where E is modulus of elasticity and ν is Poisson's ratio. Subsequently, the effective mass of delamination is given as [26].

$$M_e = \frac{9}{20}\pi\rho t a^2 \tag{2}$$

Finally, the analytical expression for calculating the LDR frequency of any defect in form of delamination is obtained by substituting Eqs. (**1**) and (**2**) in natural frequency relation of the structure, and is expressed as [26]

$$f_{LDR} = \frac{6.4t}{a^2}\sqrt{\frac{E}{12\rho(1-\nu^2)}} \tag{3}$$

Where ρ is mass density of the material.

2.2 LDR based vibro-thermography

The excitation of a structure having delamination with the LDR frequency corresponding to its damage leads to a rise in temperature at the defect location, as discussed previously. The heat generated at the defect location due to clapping and rubbing phenomena at the defect interface propagates away from the defect layer towards the surface of the structure. These thermal signatures are captured by using IR imaging and the technique is called as LDR based vibro-thermography. In this chapter, the LDR based vibro-thermography will be discussed by carrying out a
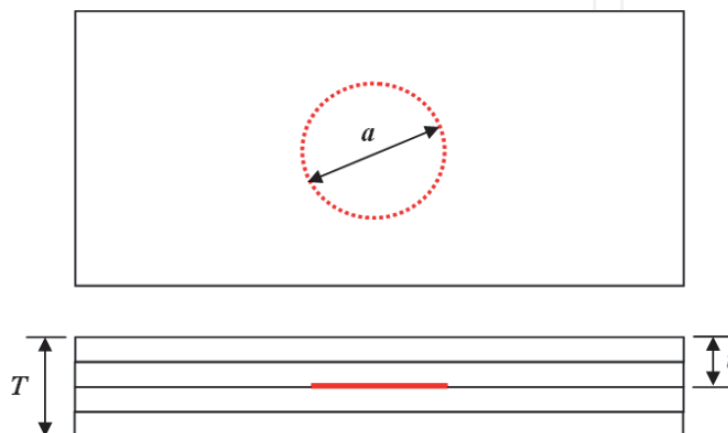
Figure 1.
Schematic of a four layered composite structure with circular delamination at the central layer.

explicit coupled temperature-displacement analysis. The nonlinear wave propagation analysis is carried out on glass fibre reinforced polymer (GFRP) composite in order to obtain the thermal response of the structure at the defect interface. The numerical model considered must fulfil the equilibrium condition in the deformed structure to obtain the solution of forces and displacements at specific nodes. The momentum equation based on principal of virtual displacement can be used for translation and rotational motion of the body under harmonic loading, and is given as [25].

$$\int_{\xi} \delta d \ \sigma d\xi + \int_{\xi} \delta v \ \rho \dot{v} d\xi + \int_{\xi} \delta v \ B d\xi - \int_{\varphi} \delta v \ S_t \ d\varphi = 0 \tag{4}$$

where ξ is current domain, φ is boundary of the body, δd is the virtual displacement, σ is stress, δv is virtual velocity, B is the body force vector and S_t is the surface traction. These terms represent the internal forces on the system, inertia force, body force and surface traction in the system, respectively.

The Courant-Friedrichs-Levy condition is satisfied while carrying out the explicit temperature-displacement analysis that requires integrating through small time increments [27]. The central-difference and forward-difference are required to be stable and hence a limit of time increment is chosen as

$$\Delta t \leq \min . \left(\frac{2}{\omega_{max}}, \frac{2}{\lambda_{max}} \right) \tag{5}$$

Where ω_{max} is highest natural frequency of the structure and λ_{max} is largest eigenvalue for the solution. The time increment, Δt must be calculated such that the wavelength does not exceed more than a single element edge length. Therefore, the size of element and time increment during the temperature-displacement analysis is a critical factor that needs to be taken care of. Otherwise, higher time increment will lead to high amplitude oscillation of the time history variables and an unstable solution.

During the coupled temperature-displacement analysis, internal stress and strain are developed due to harmonic excitations from the incident wave which further results in temperature rise at the defect location. The transient heat transfer occurring at the defect surface is computed using the following equation [25].

$$\rho C_p \frac{\partial T}{\partial t} = \nabla \phi + H_g \tag{6}$$

Where C_p is specific heat capacity, T is time dependent temperature field, ϕ is heat flux vector per unit volume and H_g is total internal heat generated per unit volume. From the Fourier's heat conduction law, the time dependent temperature during each time step can be calculated which is discretised and expressed as [25].

$$T_{n+1} = \left(\frac{C_n}{\Delta t} + \gamma_n \right)^{-1} \left(F_n + T_n \frac{C_n}{\Delta t} \right) \tag{7}$$

Where n is the analysis step (n = 1, 2, 3, ...), C is heat capacity matrix, γ is conductivity matrix and F is thermal force vector. The temperature rise at the defect location due to internal heat when the plate is excited at LDR frequency can be evaluated using the above equation. Therefore, vibro-thermography can be performed on a structure by incorporating LDR excitations that lead to higher amplitude of vibration at defect area causing a temperature rise.

3. Numerical analysis

This section discusses the numerical simulation carried out for detection of sub-surface delamination in a four layered GFRP plate with circular delamination at the central layer. The numerical model of the delaminated GFRP plate was carried out using ABAQUS 6.14 software. Each layer of the GFRP plate is considered to be of 0.5 mm thickness with the total thickness of plate as 2 mm. The area of the plate considered for numerical simulation is 180 × 180 mm² with a delamination between second and third layer. Thus, the residual thickness of the damage required for calculation of analytical LDR frequency is 1 mm. The diameter of the circular delamination is taken as 12 mm while the location of the delamination is at x = 120 mm and y = 60 mm, taking left bottom corner of the plate as the origin. **Figure 2** shows the schematic of the delaminated plate with circular delamination.

The material properties of GFRP plate used for carrying out the explicit temperature displacement analysis are given in **Table 1**. The rule of mixtures was implemented for calculating the material properties of GFRP specimen from the individual property of glass fibre and epoxy [29]. The simulation is carried out by providing sliding contact interaction properties at the defect interface. Moreover, the friction properties are included on the delamination area while the rest of the plate area is provided with tie constraints for all layers. The initial
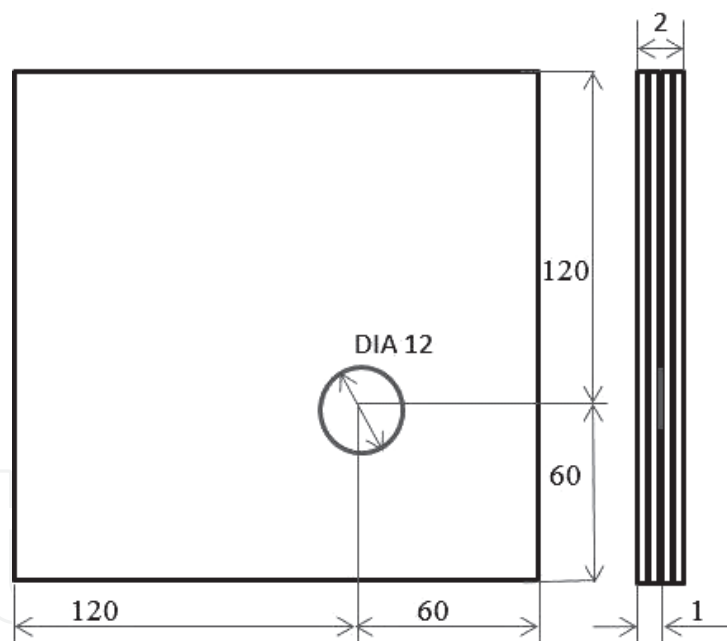
Figure 2.
Schematic of GFRP plate with circular delamination at the central layer.

Material	Density (in kg/m³)	Young's Modulus (in GPa)	Poisson's ratio	Specific heat (J/kg K)	Thermal conductivity (W/m K)
Epoxy	1200	3.30	0.35	1100.0	0.17
E-glass fibre	2540	28.0	0.22	800.81	1.35
GFRP plate	2145	10.7	0.30	908.25	0.94

Table 1.
Material properties for GFRP plate [28].

ambient temperature was considered as 293 K for all nodes of the plate. The number of elements considered for carrying out the present numerical investigation is 42,269 10-noded tetrahedral elements. First, the analytical LDR frequency of the delamination is calculated from the relation presented in previous section, followed by the steady state dynamic analysis to confirm the LDR frequency. The steady state analysis is performed on a frequency limit such that the analytical LDR calculated falls within the range of the analysis. The mode shape obtained from the contour plot of steady state analysis confirms the exact LDR frequency required for performing explicit temperature-displacement analysis. Subsequently, the explicit coupled temperature-displacement analysis is carried out followed by heat transfer analysis to detect the defect using LDR based vibro-thermography.

The explicit coupled temperature-displacement analysis is performed on the GFRP plate using single periodic LDR excitation confirmed from the steady state analysis. The force amplitude for carrying out the analysis is taken as 50 N in the thickness direction. The excitation time of 10 ms is used for vibrating the plate at its LDR frequency with a fixed time increment of 5×10^{-8} s. The time increment is calculated according to the CFL condition for explicit analysis [27]. The 10-noded modified thermally coupled second order tetrahedron (C3D10MT) mesh elements are used for the analysis. Subsequently, a node on the top surface of the plate positioned at centre of the damage area is selected to determine the amplitude of vibration during excitation. In the analysis history output, nodes at delamination layer are selected for plotting temperature profiles. The temperature gradient obtained at the end of explicit coupled temperature-displacement analysis is further used as predefined field for a heat transfer analysis. Finally, a 10 ms heat transfer analysis is performed with 10-noded quadratic heat transfer tetrahedron (DC3D10) mesh type for this step. The transient response of the heat transfer step is captured at the delamination layer as well as the top surface of the plate.

4. Results and discussions

This section discusses the results obtained from explicit coupled temperature-displacement analysis followed by heat transfer analysis in case of LDR frequency excitation based vibro-thermography. First, a steady state analysis of the GFRP plate is performed with a frequency range around the analytical LDR frequency calculated using Eq. (3). The mode shape confirming the LDR frequency of the delamination is found to be 24.8 kHz from the steady state analysis, as shown in **Figure 3**. The LDR frequency excitation in form of single periodic continuous excitation is applied on the transmitter nodes of the numerical model from the top surface.

On performing the explicit coupled temperature-displacement analysis, the amplitude-frequency spectra obtained from a node selected on the top surface of the plate above the delamination location is presented in **Figure 4**. The highest peak in the frequency spectra is obtained at 24.86 kHz which is close to the result obtained from steady state analysis. The highest amplitude of 6.488×10^{-6} m was observed at the delamination area.

Subsequently, the average nodal temperature profile at the delamination location during the span of explicit dynamic coupled temperature-displacement analysis is plotted in **Figure 5**. The plot shows variation of temperature at the delamination interface with respect to time of excitation. It is observed that the average nodal temperature at delamination location starts rising after 4 ms of excitation. The nodal temperature at delamination region rises gradually to around
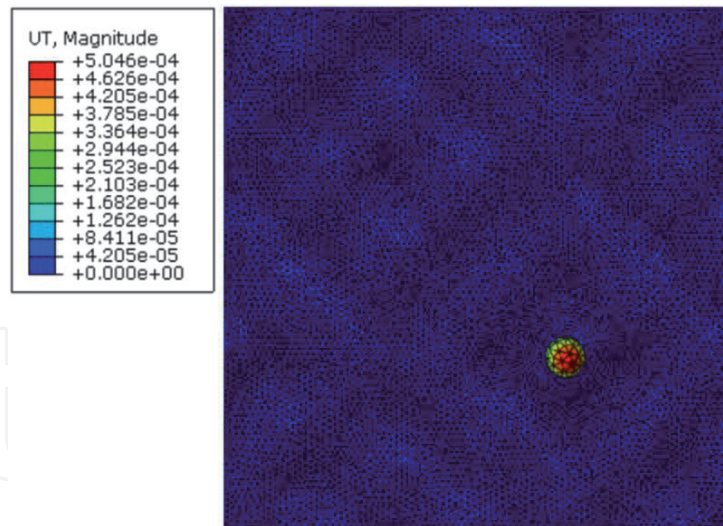
Figure 3.
*Contour plot of the GFRP plate depicting the mode shape of the delamination at LDR frequency of 24.8 kHz.*
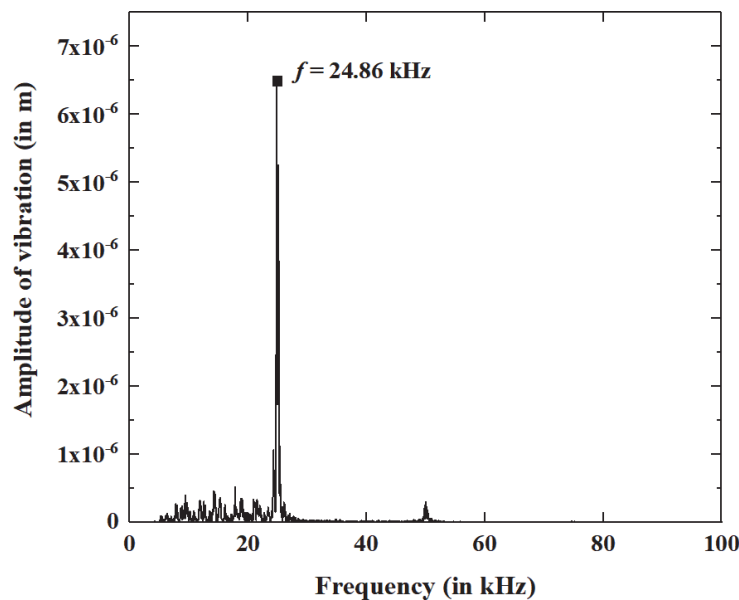
Figure 4.
Frequency spectra obtained at the delamination location on the top surface of the plate for single periodic LDR excitation.

293.015 K in 10 ms. Since, the temperature rise is not saturated at the end of excitation, the plate can be excited for more time until the temperature rise saturates.

Moreover, all the elements over the delamination area is selected to plot the elemental temperature rise over delamination during 10 ms of heat transfer analysis, as illustrated in **Figure 6**. The plot shows a rise of temperature from the ambient for some of the elements over the delamination area. It is observed that the maximum temperature recorded during heat transfer analysis is 293.15 K. Since the temperature rise over the delamination region is around 150 mK, the vibro-thermography scanning can be done at this instance of time with any IR camera that normally has a resolution of 30 mK.

Furthermore, contour plot for nodal temperature on the delamination surface of GFRP plate after explicit temperature-displacement analysis is illustrated in **Figure 7**. It is clear from the contour plot that the temperature rise is observed only
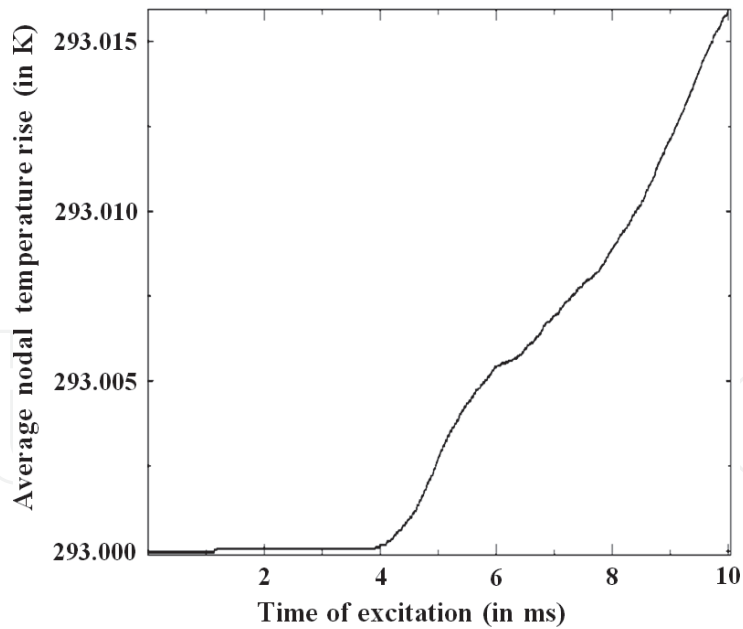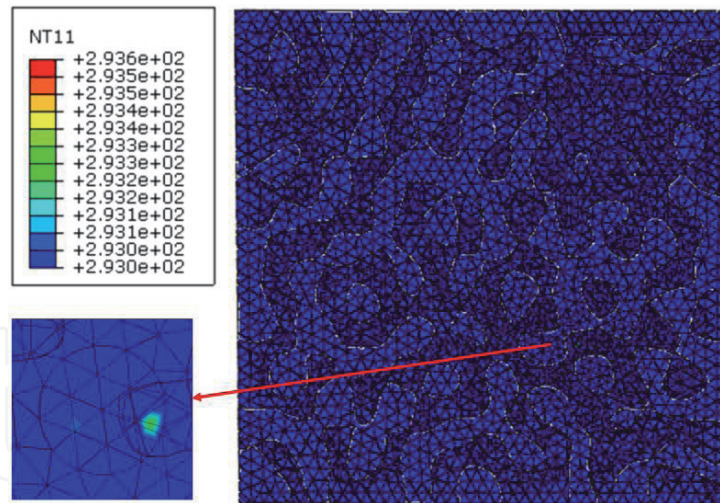
Figure 5.
*Average nodal temperature rise at delamination layer for single periodic continuous LDR excitation.*
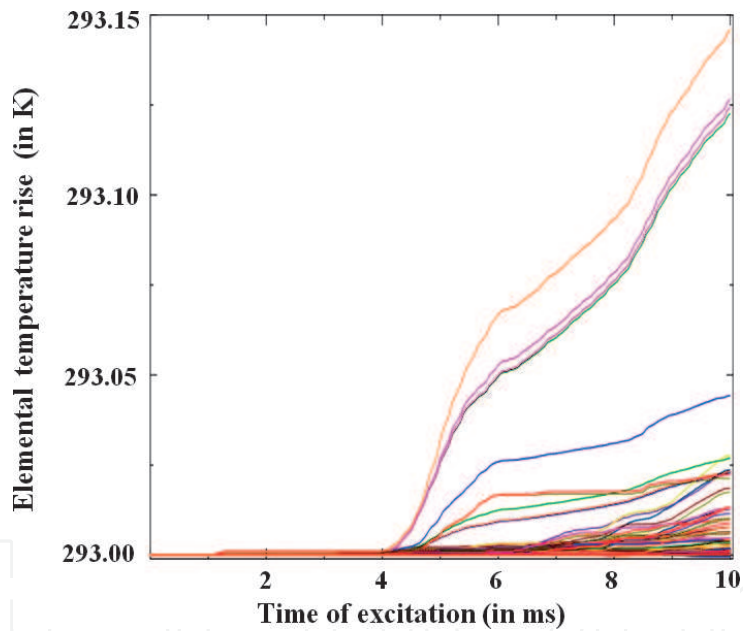
Figure 6.
Elemental temperature rise at delamination layer for single periodic continuous LDR excitation.

at the delamination location while the rest of the plate shows no thermal signatures at all. However, it is clear that the whole delamination area is not covered by the heat flow at this time instance. Hence, the excitation of the plate must be done for more time period such that the whole delamination area is covered by the heat distribution. Similarly, the elemental temperature is shown in contour plot depicted in **Figure 8**, where heat is distributed to a larger area after heat transfer analysis as compared to the explicit temperature-displacement analysis. Although, the whole delamination is not covered at this instance and more time for excitation is required. The defect imaging at later time increment is advantageous because of better judgement and idea of defect shape and size is detected easily. This is one of the merits of performing LDR based vibro-thermography technique that provides high contrast defect images that can be captured using an IR camera.

Figure 7.
Contour plot of nodal temperature on the delamination surface of delaminated GFRP plate after heat transfer analysis.
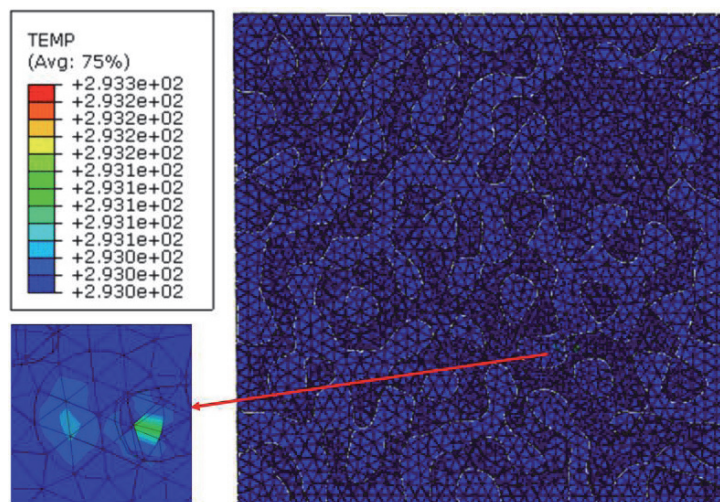
Figure 8.
Contour plot of nodal temperature on the top surface of delaminated GFRP plate at 10 ms during single periodic continuous LDR excitations.

5. Conclusions

In this chapter, a LDR frequency excitation based vibro-thermography technique is implemented for detection of a circular delamination in a four layered GFRP plate. The analytical LDR frequency is calculated using the expression discussed in the theory section. The analytical LDR frequency is then confirmed by carrying out a steady state dynamic analysis. The mode shape obtained from the contour plot of the steady state analysis confirms the LDR frequency of the delamination which is further used for carrying out the explicit dynamic coupled temperature-displacement analysis. Subsequently, the amplitude-frequency spectra during the temperature-displacement analysis is plotted to observe a rise in temperature at the defect location due to clapping and rubbing action during resonance. The average nodal at delamination layer is presented to find the maximum temperature rise at delamination region when the plate is excited with LDR frequency. Moreover, a 10 ms heat transfer analysis is carried out to obtain high contrast temperature response on top surface of the GFRP plate. Finally, the temperature profile is plotted for all elements over the delamination layer after heat transfer

analysis. The temperature profile plotted at the defect interface signifies that the temperature rises drastically when the structure is excited with LDR frequency and subsequently, enhances the chance of defect detection using vibro-thermography technique. The vibro-thermographic imaging using an IR camera is recommended after longer period of LDR excitation. Thus, the LDR based vibro-thermography is found to be an efficient tool for detection, location and size estimation of defects in composite structures.

Author details

Subhankar Roy and Tanmoy Bose*
Department of Mechanical Engineering, National Institute of Technology
Meghalaya, Shillong, Meghalaya, India

*Address all correspondence to: tanmoy.jgec04@gmail.com

IntechOpen

References

[1] Henneke EG, Reifsnider KL, Stinchcomb WW. Thermography—An NDI method for damage detection. The Journal of the Minerals, Metals & Materials Society. 1979;**31**(9):11-15

[2] Pye CJ, Adams RD. Detection of damage in fibre reinforced plastics using thermal fields generated during resonant vibration. NDT International. 1981;**14**(3):111-118

[3] Rantala J, Wu D, Busse G. Amplitude-modulated lock-in vibrothermography for NDE of polymers and composites. Research in Nondestructive Evaluation. 1996;7: 215-228

[4] Wu D, Busse G. Lock-in thermography for nondestructive evaluation of materials. Revue Générale de Thermique. 1998;**37**(8):693-703

[5] Han X, Zeng Z, Li W, Islam Md S, Lu J, Loggins V, et al. Acoustic chaos for enhanced detectability of cracks by sonic infrared imaging. Journal of Applied Physics. 2004;**95**(7):3792-3797

[6] Renshaw J, Holland SD, Thompson RB. Measurement of crack opening stresses and crack closure stress profiles from heat generation in vibrating cracks. Applied Physics Letters. 2008;**93**(8):081914

[7] Junyan L, Qingju T, Yang W. The study of inspection on SiC coated carbon–carbon composite with subsurface defects by lock-in thermography. Composites Science and Technology. 2012;**72**(11): 1240-1250

[8] Mendioroz A, Castelo A, Celorrio R, Salazar A. Characterization of vertical buried defects using lock-in vibrothermography: I. Direct problem. Measurement Science and Technology. 2013;**24**(6):065601

[9] Castelo A, Mendioroz A, Celorrio R, Salazar A. Optimizing the inversion protocol to determine the geometry of vertical cracks from lock-in vibrothermography. Journal of Nondestructive Evaluation. 2017; **36**(1):3

[10] Ciampa F, Mahmoodi P, Pinto F, Meo M. Recent advances in active infrared thermography for non-destructive testing of aerospace components. Sensors. 2018;**18**(2):609

[11] He Y, Chen S, Zhou D, Huang S, Wang P. Shared excitation based nonlinear ultrasound and vibrothermography testing for CFRP barely visible impact damage inspection. IEEE Transactions on Industrial Informatics. 2018;**14**(12): 5575-5584

[12] Derusova DA, Vavilov VP, Guo X, Druzhinin NV. Comparing the efficiency of ultrasonic infrared thermography under high-power and resonant stimulation of impact damage in a CFRP composite. Russian Journal of Nondestructive Testing. 2018;**54**(5): 356-362

[13] Derusova DA, Vavilov VP, Guo X, Shpil'noi VY, Danilin NS. Infrared thermographic testing of hybrid materials using high-power ultrasonic stimulation. Russian Journal of Nondestructive Testing. 2018;**54**(10): 733-739

[14] Geetha GK, Mahapatra DR. Modeling and simulation of vibro-thermography including nonlinear contact dynamics of ultrasonic actuator. Ultrasonics. 2019;**93**:81-92

[15] Poelman G, Hedayatrasa S, Segers J, Van Paepegem W, Kersemans M. Adaptive spectral band integration in flash thermography: Enhanced defect detectability and quantification in

composites. Composites Part B: Engineering. 2020;**202**:108305

[16] Poelman G, Hedayatrasa S, Segers J, Van Paepegem W, Kersemans M. An experimental study on the defect detectability of time- and frequency-domain analyses for flash thermography. Applied Sciences. 2020;**10**(22):8051

[17] Solodov I, Bai J, Busse G. Resonant ultrasound spectroscopy of defects: Case study of flat-bottomed holes. Journal of Applied Physics. 2013;**113**(22):223512

[18] Lima WJND, Hamilton MF. Finite-amplitude waves in isotropic elastic plates. Journal of Sound and Vibration. 2003;**265**:819-839

[19] Ciampa F, Pickering SG, Scarselli G, Meo M. Nonlinear imaging of damage in composite structures using sparse ultrasonic sensor arrays: Nonlinear imaging of damage. Structural Control and Health Monitoring. 2017;**24**(5): e1911

[20] Fierro GPM, Ginzburg D, Ciampa F, Meo M. Imaging of barely visible impact damage on a complex composite stiffened panel using a nonlinear ultrasound stimulated thermography approach. Journal of Nondestructive Evaluation. 2017;**36**(4):69

[21] Solodov I, Bai J, Bekgulyan S, Busse G. A local defect resonance to enhance acoustic wave-defect interaction in ultrasonic nondestructive evaluation. Applied Physics Letters. 2011;**99**(21):211911

[22] Razani M, Parkhimchyk A, Tabatabaei N. Lock-in thermography using a cell phone attachment infrared camera. AIP Advances. 2018;**8**:035305

[23] Solodov I, Derusova D, Rahammer M. Thermosonic Chladni figures for defect-selective imaging. Ultrasonics. 2015;**60**:1-5

[24] Rahammer M, Kreutzbruck M. Fourier-transform vibrothermography with frequency sweep excitation utilizing local defect resonances. NDT & E International. 2017;**86**:83-88

[25] Fierro GPM, Calla D, Ginzburg D, Ciampa F, Meo M. Nonlinear ultrasonic stimulated thermography for damage assessment in isotropic fatigued structures. Journal of Sound and Vibration. 2017;**404**:102-115

[26] Solodo I, Rahammer M, Gulnizkij N, Kreutzbruck M. Noncontact sonic NDE and defect imaging via local defect resonance. Journal of Nondestructive Evaluation. 2016;**35**(3):48

[27] Courant R, Friedrichs K, Lewy H. On the partial difference equations of mathematical physics. IBM Journal of Research and Development. 1967;**11**(2): 215-234

[28] AZo Materials—Online Publication for Materials Science Community [Internet]. Available from: https://www.azom.com/properties.aspx?ArticleID= 764 [Accessed: 11 October 2021]

[29] Liu GR. A step-by-step method of rule-of-mixture of fiber- and particle-reinforced composite materials. Composite Structures. 1998;**40**(3–4): 313-322